ELSEVIER

Thermochimica Acta 289 (1995) 327–341

thermochimica acta

An advanced calorimetric approach for population balance modelling in batch crystallization processes [1]

O. Monnier [a], G. Févotte [b], C. Hoff [a], J. P. Klein [b]

[a] *SANOFI CHIMIE, Route d'Avignon, 30390 Aramon, France*
[b] *LAGEP URA CNRS D1328, Université Claude Bernard Lyon 1, CPE-Lyon. Bat. G308, 43 bd du 11 Novembre 1918, 69622 Villeurbanne Cedex, France*

Received 12 December 1995; accepted 28 March 1996

Abstract

For most batch crystallization processes, it remains difficult to obtain on-line relevant information about both the dissolved solid concentration in the liquid phase and the crystal size distribution (CDS). Consequently, very few studies dealing with the estimation of crystallization kinetics, i.e. primary and secondary nucleation rates and growth rates, can be found in the literature. Moreover, the reported experimental results are generally based upon simplified population balance models, such as moment equations which are known to contain insufficient information on the CSD.

Therefore, the aim of this article is to present a new technique for flexible process-measurement and modelling during batch cooling crystallizations. Measurements of supersaturation were ensured by using the Mettler RC1 calorimeter which has been coupled with an on-line insitu laser sensor. Final CSD measurements have been achieved through image analysis. In addition to this measurement strategy, the population balances were solved to simulate the time variations of the CSD.

In order to evaluate the method, isothermal adipic acid/water crystallizations have been performed. These experiments allowed selection of the crystallization kinetic model and estimation of the corresponding parameters. Comparisons between experimental and simulated variables, such as the supersaturation, the heat release due to the crystal growth and the final CSD, are satisfactory.

Keywords: Crystal size distribution; Kinetic modelling; Numerical simulation; Reaction calorimetry; Solution crystallization

* Corresponding author. Fax: 78 94 0962

[1] This paper is a contribution to the special thematic issue "Reaction Calorimetry", edited by Ralph N. Landau.

PII S0040-6031(96)03010-9

1. Introduction

Crystallization from solution is an important separation and purification unit operation in the field of chemical engineering and can be used to obtain solid products of high purity at low costs. In the field of fine chemistry (pharmaceuticals, agrochemicals, photographic films, etc.), batch crystallization operations are employed to obtain high value-added products which are essentially characterized by their crystal size distribution (CSD). In an industrial context, mastery of the CSD, and notably the improvement of process reproducibility, is a key issue since most quality requirements and end-use properties of the crystals are strongly dependent on the CSD. For example, the ease of filtration, the flow characteristics, or the chemical purity of the particles may be severely impaired if excessive amounts of fines have been generated during the batch operation. The course of supersaturation is known to effect considerably the final CSD, and, in the case of batch processes, it is worth noting that the width of the CSD generally tends to increase in an undesirable fashion as a function of time. Consequently, the automatic closed-loop control of industrial crystallizers, or, at least the open-loop optimization of operating conditions, is of potentially great importance. Indeed, regardless of the control algorithm envisaged, a necessary requirement is that on-line measurements relating the time variations of relevant output variables such as CSD or supersaturation be available.

From that point of view, two distinct categories of instruments can be defined, according to the information which they provide. Particle size analysers would obviously be useful for the monitoring of crystal quality, and for the detection of the onset of particular phenomena such as delayed nucleations, or insufficient crystal growth. In addition to such measurements, it is essential to control the course of supersaturation which is the driving-force of any elementary crystallization process.

In an industrial context, where only a short time might be devoted to the development of the manufacturing process of pharmaceutical molecules, it is of major importance to design efficient methods for improving the quality and reproducibility of low tonnage, multipurpose productions. The principal objective of the work described in this article is to present a new technique for flexible process-measurement and modelling during batch cooling crystallizations. A calorimetric method is proposed as an indirect supersaturation sensor. Two different techniques are also applied for the determination of CSD. For that purpose, the performance of an insitu laser sensor is compared with results obtained through off-line image analysis. In order to evaluate different kinetic models, isothermal crystallization experiments of adipic acid in water have been performed with low solids content. A satisfactory fit between the experimental calorimetric and CSD data, and simulated data was obtained.

2. Experimental setup

2.1. Dissolved solid concentration measurements

Several methods and devices can be envisaged for the on-line measurement of supersaturation. For example, it can be determined from the density of the crystal-free

solution [1]. For modelling and control purposes, Miller and Rawlings [2] used an on-line densitometer, and these authors consider the technique as routine and reliable. Qui and Rasmuson [3] also measured the concentration of succinic acid in water by using a densitometer. However, it should be noted that the requirement for an external sampling loop is likely to entail various operating difficulties. In particular, the sample stream should be maintained free of solids by some appropriate screen, and a heat exchanger is necessary to keep the measurement loop as isothermal as possible. Moreover, density measurements are not accurate in the case of industrial solutions with variable concentrations of impurites, which is the case for most pharmaceutical processes. It has been proposed by some authors that the conductivity of crystallizing solutions be measured to assess the dissolved solid concentration [4, 5]. Even though no external sampling device is necessary in this case, several major limitations should be noted : the method is generally unsuitable for organic systems; very large measurement errors occur when undesirable crystallization (fouling) takes place on the conductivity cell; the results are temperature-dependent and senstitive to possible impurities, and, therefore, careful calibration procedures must be performed.

2.2. *A calorimetric approach for continuous phase measurements during crystallization*

As an on-line indirect sensor, calorimetry is, in theory, a rather straight forward technique. The measured information is used to deduce the heat of crystallization, and thus the rate of crystal growth. To the best of our knowledge, only a few applications of calorimetry as a tool for monitoring crystallization operations have been reported in the literature. Riesen [6] used the RC1 Mettler reaction calorimeter for monitoring and optimizing batch solution crystallizations. An automated procedure for the determination of solubility curves was presented and turbidimetry was proposed as an additional sensor. This last article is more qualitative than quantitative in terms of the specific case of crystallization processes since no equations explaining the method are presented. However the application was very encouraging. König et al. [7] developed a very simple calorimeter where only the crystallization temperature is measured. Off-line calculations of supersaturation and their possible use in kinetic modelling were briefly described, but the approach remained succint. An adaptive strategy based on the joint use of on-line calorimetry and the so-called Partial State Model Reference Generalized Predictive Control algorithm (PSMR GPC) was reported [8]. This study was motivated by industrial safety requirements concerning the supervision of the unpredictable exothermal phenomenon of primary nucleation. In another article, the possibility of using calorimetric estimates for the analysis of important features of crystallization processes, such as operating uncertainties related to unseeded batch crystallizations, qualitative assessment of seeding policies, quantitative relationships between seeding supersaturation and the thermal effects of the initial growth of nuclei, was considered [9]. A calorimetric procedure for the off-line measurement of supersaturation was also described, and encouraging experimental results have been obtained in the context of batch evaporative multipurpose crystallizations [10].

No study dealing with the joint use of calorimetry and CSD measurements to fit kinetic and population balance models has yet been published for crystallization

processes. In order to fill this void, a Mettler RC1 reaction calorimeter was used in an experimental study. Details of this system may be found in numerous articles, and will therefore not be discussed here. If it is assumed that the molar enthalpy of crystallization. ΔH_C, is constant, one can compute the mass of crystallized solid $m_C(t)$ from the measured profiles of the instantaneous power of the "reaction" (refered to as $Q_{cryst}(t)$ below), and therefore estimate the relative supersaturation $\beta(t)$ (see the Nomenclature for the meaning of the symbols)

$$m_C(t) = \int_{t_o}^{t} \frac{M Q_{cryst}(t)}{V_T(t)|\Delta H_C|} dt \tag{1}$$

and

$$\beta = \frac{C(t)}{C^*(T(t))} = \frac{(m_0 - m_C(t))}{M C^*(T(t))} \tag{2}$$

As an example, estimates of the instantaneous power of crystallization $Q_{cryst}(t)$ and of the relative supersaturation are displayed in Fig. 1. These data were obtained off-line from the unseeded batch crystallization of adipic acid in water. The initial solution was cooled from 70°C to the limit of the metastable zone where primary nucleation took place, following which the contents of the crystallizer were maintained at a constant temperature. It clearly appears that primary nucleation is followed by a sharp thermal effect together with a decrease of $\beta(t)$ towards its equilibrium value, $\beta = 1$.

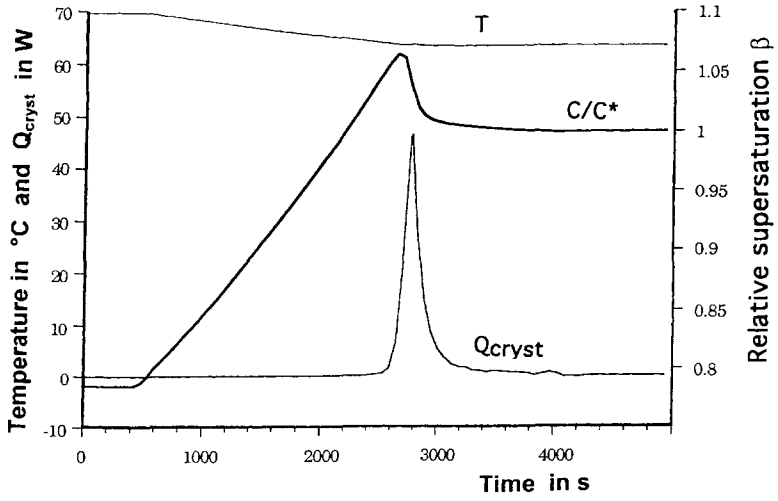

Fig. 1. Typical supersaturation and Q_{cryst} profiles obtained after batch crystallization performed in the RC1 calorimeter.

2.3. Laser CSD measurements

As clearly demonstrated by some authors [2,11], CSD measurements are required for reliable modelling and parameter estimation of crystallizers, and for their feedback control. From that point of view, the advent of laser-measurement techniques appeared to be extremely promising, as very few particle size analysers or counting systems available on the market offer the possibility of continuous in situ monitoring of CSD during crystallization operations. Unfortunately, as outlined in the recent review paper by Rawlings et al. [12], the technique does not work without stringent restrictions. The analytical equations referred to as Mie theory can be solved for optically smooth spherical particles, but apply poorly to irregular crystal shapes. However, for relatively large particles, the Fraunhofer diffraction approximation can be used, but the estimation of populations of small crystals generally appears to be unsatisfactory. Moreover, in order to compute the CSD from the recorded scattered laser light, it is necessary to solve a highly ill-conditioned inverse problem which means that large uncertainties generally remain.

Among the relatively high number of commercially available CSD sensors operating on different principles, much interest has been aroused by the appearance of the ParTec® 100 analyser patented by Laser Sensor Technology Inc [13, 14]. The design of this instrument is such that its laser probe can be placed in the slurry without the need for sampling and dilution systems; 38 size-ranges are covered from 1.9 to 1000 μm. The light beam emitted by a laser diode is focused on a focal point in the suspension, close to the probe, as shown in Fig. 2. The focusing lens is subjected to an eccentric rotation

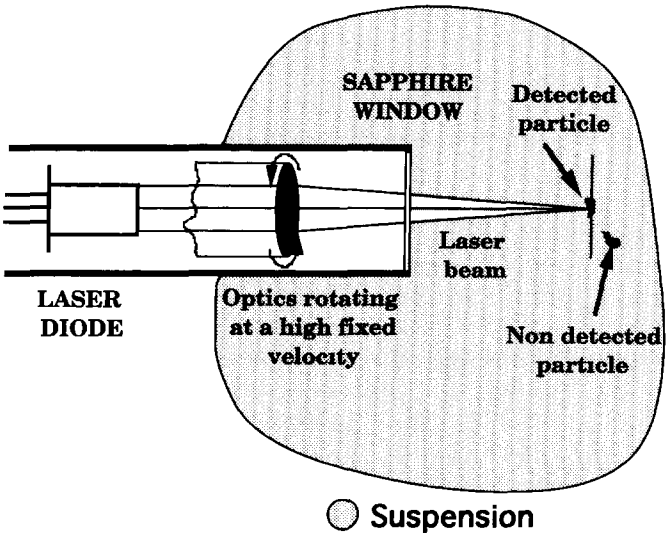

Fig. 2. Schematic representation of the in situ ParTec 100 Laser sensor.

generated electromagnetically that causes the focal point to be displaced in a circular pattern, the amplitude depending on the distance from the focal point to the probe. The optical pulses which originate from reflections of the probe light on the particles are collected and passed via a fiber optic cable to the detector. A discrimination loop sorts impulse for short rise time. All particles passing elsewhere than in the focal plane give pulses of longer rise time, and are thus eliminated. The focal spot is scanned at constant rotational speed (4410 rpm) so that the time the laser beam takes to scan the particle, and thus the reflection time, are direct functions of the distribution segments of these surface sizes registers an increment when a determination takes place between the boundaries of the corresponding segment. At the end of the cycle, a size distribution histogram is reconstructed in terms of percentages of particle counts.

A study has been carried out to verify the accuracy and reproducibility of particle size measurements, and to elucidate the influence of experimental parameters on the output data [15]. It appears that most CSD determinations are influenced by a large number of operating variables. In particular, the optimal focal point position was found to be largely size-dependent, especially in the case of small particles. Consequently, an instrument that requires different focal point settings for precise analysis of dispersed samples does not seem to be suitable for large distributions. Roughly speaking, and irrespective of the product of concern, large sizes were rather underestimated while small particles were overestimated.

2.4. CSD image analysis measurements

It turns out that off-line Image Analyses(IA) can provide satisfactory information on the CSD of the product, and can be used to overcome some of the difficulties associated with the use of laser sensors. Samples are placed under the microscope on an automated bench. Before being numerized into a square pixel network by the system, the image is acquired by a CCD video camera (Charged Couple Device). Random displacements of the bench are controlled by the panel keys. The sets of resulting images are processed by the image analyser connected to a personal computer. The technology of the image analyser is based on the use of specialized processors that provide very fast treatments, sometimes to the detriment of flexibility. Many standard IA software packages are available for this purpose. The microcomputer is also dedicated to various storage, processing and printing functions required by the study. Three different directions were used to measure the size of a given particle, and an average diameter was then calculated from these 3 values. The reproducibility of the method, assessed experimentally, has been found satisfactory. Unless very complex crystal morphologies are involved, only 500–1000 particles are required to provide a correct representation of the population. Experimental results such as those displayed in Fig. 3 demonstrate the existence of major differences between the results obtained from laser measurements and those from image analyses. As expected from preliminary experiments, the Lasentec distribution was abnormally broader than that obtained from IA. The latter was finally selected to provide reliable CSD information.

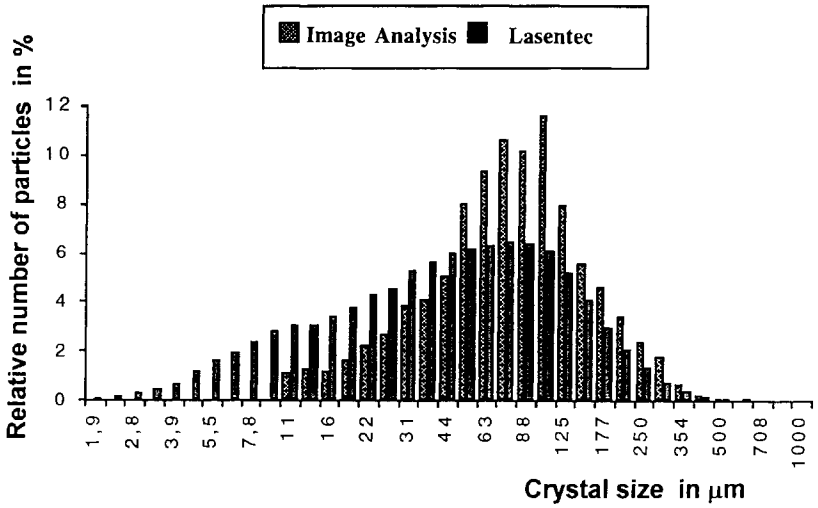

Fig. 3. Comparison between image analysis and Lasentec CSD measurements.

2.5. *Coupling the laser CSD sensor with the Mettler RC1 reaction calorimeter*

Despite the limitations of the CSD laser sensor, it might be of great interest to use it for monitoring (at least qualitatively) the onset of particular phenomena such as primary and secondary nucleations. For that purpose, the ParTec 100 analyser was coupled with the Mettler RC1 calorimeter. As an example, typical experimental data are displayed in Fig. 4. During this almost isothermal experiment, a known almost of adipic acid was dissolved in water in order to determine the enthalpy of dissolution. Before the experiment, both the calorimeter and the crystals of adipic acid were heated to 50°C. At time 600 s, the thermal effect of the dissolution is clearly observed through the course of the instantaneous power $Q_{cryst}(t)$ together with the fast increase of the particle number which may easily be explained since the final dissolution follows a phase of separation of initial larger agglomerated particles. The energy consumption associated with the solid dissolution was followed by a transient temperature decrease.

3. Modelling and numerical simulation of crystallizations

3.1. *Experimental design*

Distilled water and adipic acid were weighed and introduced into the calorimeter at ambient temperature. Dissolution was ensured through a programmed heating ramp. The effect of stirring is known to be rather complex. In order to reduce attrition and breakage, on the one hand, and to obtain sufficient homogeneity and good heat

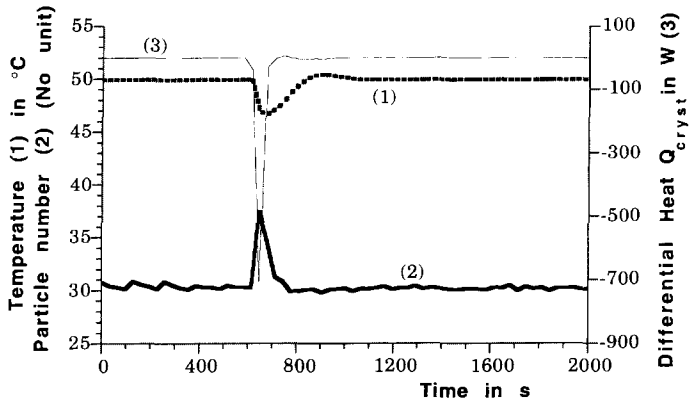

Fig. 4. Joint use of calorimetry and of laser CSD measurements: example of the isothermal determination of dissolution enthalpy.

transfer, on the other, good circulation should be maintained in the crystallizer, while shear stress has to be minimized. An acceptable compromise was observed through the use of axial flow profiled propellers (Mixel TT). Constant cooling slopes were imposed ($-10°C\,h^{-1}$) between the initial temperature outside the metastable zone and the primary nucleation temperature. Once the total number of counts of the laser sensor reached a prespecified value, i.e. above 1000 counts, the crystallizer was operated under isothermal conditions. The process was terminated when the crystal growth had consumed all of the accumulated supersaturation. The moderate amount of crystals obtained with this method allowed us to reduce both attrition, breakage, and agglomeration.

3.2. Population balance modelling

The population of crystals during the batch process is described by the density function ψ. For the sake of simplicity, it is assumed that only one size dimension L is sufficient for the characterization of the crystals. Therefore, $\psi(L, t)\mathrm{d}L$ is the number of crystals of size between L and $L+\mathrm{d}L$ per unit volume, at time t. Then, during the interval $\mathrm{d}t$, the balance of crystals in the size interval $[L, L+\mathrm{d}L]$ can be written as follows

$$\frac{1}{V_T(t)}\frac{\partial}{\partial t}[\psi(L, t)V_T(t)] = -\frac{\partial}{\partial L}[G(L, t)\psi(L, t)] \tag{3}$$

with the boundary condition

$$\psi(L_0, t) = \frac{r_{N1}(L_0, t) + r_{N2}(L_0, t)}{G(t)|_{L=L_0}} \tag{4}$$

Eq. (4) expresses possible primary and secondary nucleations as the generation of new crystals of critical size L_0 upon formation, where $[0, L_0]$ is the smallest class considered in the population balance. In our case, primary heterogeneous nucleation was assumed to initiate the crystallization according to the following kinetic

$$r_{N1} = A \exp(-B/\ln^2 \beta) \tag{5}$$

where r_{N1} is the primary heterogeneous nucleation rate (number of new crystals/(s m^3)), and A, B are coefficients to be determined. Following primary nucleation, secondary nucleation might take place; the rate r_{N2} was assessed from Eq. (6) which is similar to Eq. (5), but accounts for the effect of the generation of crystal surface S_p

$$r_{N2} = A_{sec} S_p \exp(-B_{sec}/\ln^2 \beta) \tag{6}$$

The growth of crystals in the supersaturated solution is a complex process usually expressed in terms of the rate of variation of a characteristic crystal size, $G = dL/dt$. The film model may relate the growth as a two-fold mechanism where the solute is transported by diffusion and/or convection and integrated into the solid surface [16]. A diffusive/convective mass transfer Φ through a film around the surface of the growing crystal is assumed, between the bulk concentration C and the concentration at the crystal–solution interface, denoted C_i. The integration mechanism is represented by Φ_i, as follows

$$\Phi = k_d(C - C_i)$$

and

$$\Phi_i = k_C(C_i - C^*)^n \tag{7}$$

where k_d is the mass transfer coefficient, Φ is the flux density of the mass transfer (mol s^{-1} m^{-2}), k_C is the integration kinetic constant and n the kinetic order; k_d may be assessed from various available correlations such as the adimensional relationship of Levins and Glastonbury [17]. The calculations involved in the determination of k_d will not be discussed here.

At steady state, one may assume that all the mass transferred has been used to increase the size of the crystals so that Q_{cryst} is given by the following equation where the mass growth rate dm_C/dt may easily be computed from the growth flux density

$$Q_{cryst}(t) = \frac{dm_C}{dt} \frac{|\Delta H_C|}{M} V_T(t) \tag{8}$$

Eq. (8) provides a means of fitting the calorimetric measurements to the set of population balance equations. In particular, the simulated crystal growth should be in agreement with both the measured $Q_{cryst}(t)$ profiles, and the final CSD obtained through images analysis.

The method of classes was introduced [18] as a means of recovering without excessive simplification, the density functions through the continuous to discrete translation of the population balance. N classes $\mathscr{C}_i$ $(i = 1, N)$ of particles are defined by a suite of $N+1$ sizes : L_0, L_1 ... L_N. The characteristic size of the ith class is

$S_i = (L_{i-1} + L_i)/2$. The number of crystals per unit of volume is the class $\mathscr{C}_i$ is thus given by

$$N_i(t) = \int_{L_{i-1}}^{L_i} \psi(L, t)\mathrm{d}L \tag{9}$$

In a given class $\mathscr{C}_i$, $\psi(L, t)$ can be approximated by a constant value denoted $f_i(t)$, and it may be shown using a Taylor series expansion that $\psi(L_i)$ is well represented as the arithmetic mean of ψ on $\mathscr{C}_i$ and $\mathscr{C}_{i+1}$, i.e.

$$N_i(t) = f_i(t)(L_i - L_{i-1}) = f_i(t)\mathscr{L}_i$$

with

$$\psi(L_i) = [f_i(t) + f_{i+1}(t)]/2 \tag{10}$$

Thus, the generic approximation associated with the population balance of class $\mathscr{C}_i$ is given by Eq. (11), obtained through a Taylor-series expansion, where t should now be considered as a discrete time index

$$\frac{\mathrm{d}N_i(t)}{\mathrm{d}t} \cong \frac{1}{V_T(t)}\frac{\mathrm{d}V_T(t)}{\mathrm{d}t}N_i(t) - G(L_i, t)[\mathscr{A}(i)N_i(t) + \mathscr{B}(i)N_{i+1}(t)] + G(L_{i-1}, t)[\mathscr{A}(i-1)N_{i-1}(t) + \mathscr{B}(i-1)N_i(t) + R_{N2,i}(t) \tag{11}$$

where

$$\mathscr{A}(i) = \frac{\mathscr{L}_{i+1}(t)}{\mathscr{L}_i(t)[\mathscr{L}_i(t) + \mathscr{L}_{i+1}(t)]}$$

and

$$\mathscr{B}(i) = \frac{\mathscr{L}_i(t)}{\mathscr{L}_{i+1}(t)[\mathscr{L}_i(t) + \mathscr{L}_{i+1}(t)]} \tag{12}$$

Since all primary and secondary nucleation takes place in the first class $\mathscr{C}_1$, the nulceation terms should be defined as

$$R_{N1,i}(t) = r_{N1}(t) \quad \text{if} \quad i = 1; \quad R_{N1,i}(t) = 0 \quad \text{if} \quad i \neq 1 \tag{13a}$$

$$R_{N2,i}(t) = r_{N2}(t) \quad \text{if} \quad i = 1; \quad R_{N2,i}(t) = 0 \quad \text{if} \quad i \neq 1 \tag{13b}$$

In order to reproduce the measured CSDs, the method of moment has been applied with kinetic equations (5)–(7). The differential equations involved in the population balances were solved by using a 4th-order Runge–Kutta sub-routine. Then, by using the obtained CSDs, the total number of crystals N_T may be computed from the final mass $m_{c,f}$ of crystallized solid as follows

$$N_T \cong \frac{6}{\pi\rho_S}\frac{\alpha_v m_{c,f} V_T}{\sum_{i=1}^{N}\left[S_i^3 \dfrac{N_i}{\sum_{i=1}^{N} N_i}\right]} \tag{14}$$

In addition, the time variations of the differential heat of crystallization $Q_{cryst}(t)$ were calculated from Eq. (8). The general structure of the modelling and simulation strategy is represented by the scheme in Fig. 5.

4. Identification of batch crystallizations

4.1. Experimental results

Batch operations were carried out to determine the kinetic parameters. The final CSDs, determined by Image Analysis, and a typical example of calorimetric estimates are displayed in Fig. 6. For each batch, Eq. (14) yields a value of N_T which is used as a key parameter for the dynamic simulations of CSD. Moreover, as explained previously, calorimetric measurements are also available to calculate m_C from the enthalpy of crystallization ΔH_C and the estimated profile $Q_{cryst}(t)$). Despite the small amounts of solid involved, the final mass of solid is consistent with the observed heat

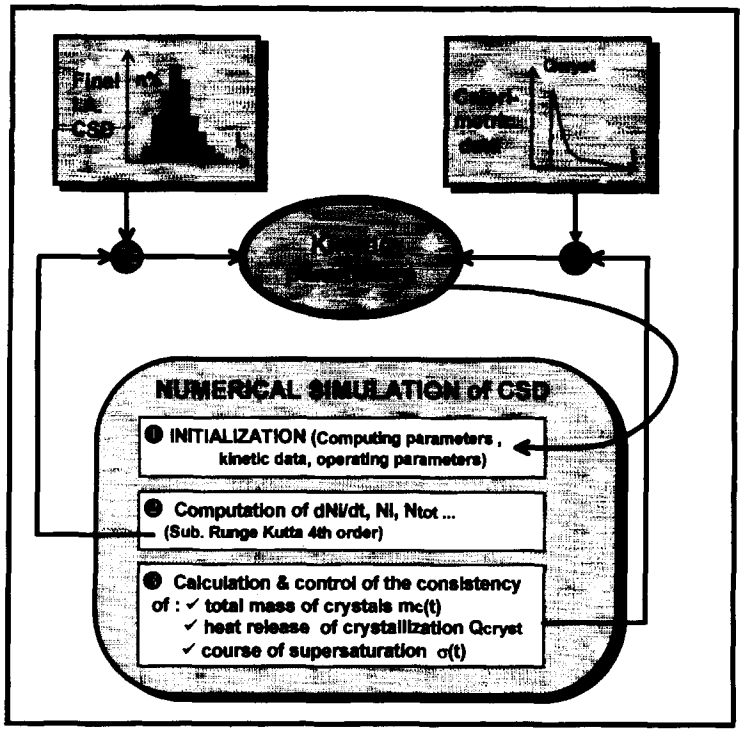

Fig. 5. Structure of the program for the simulation of population balances after batch solution crystallizations.

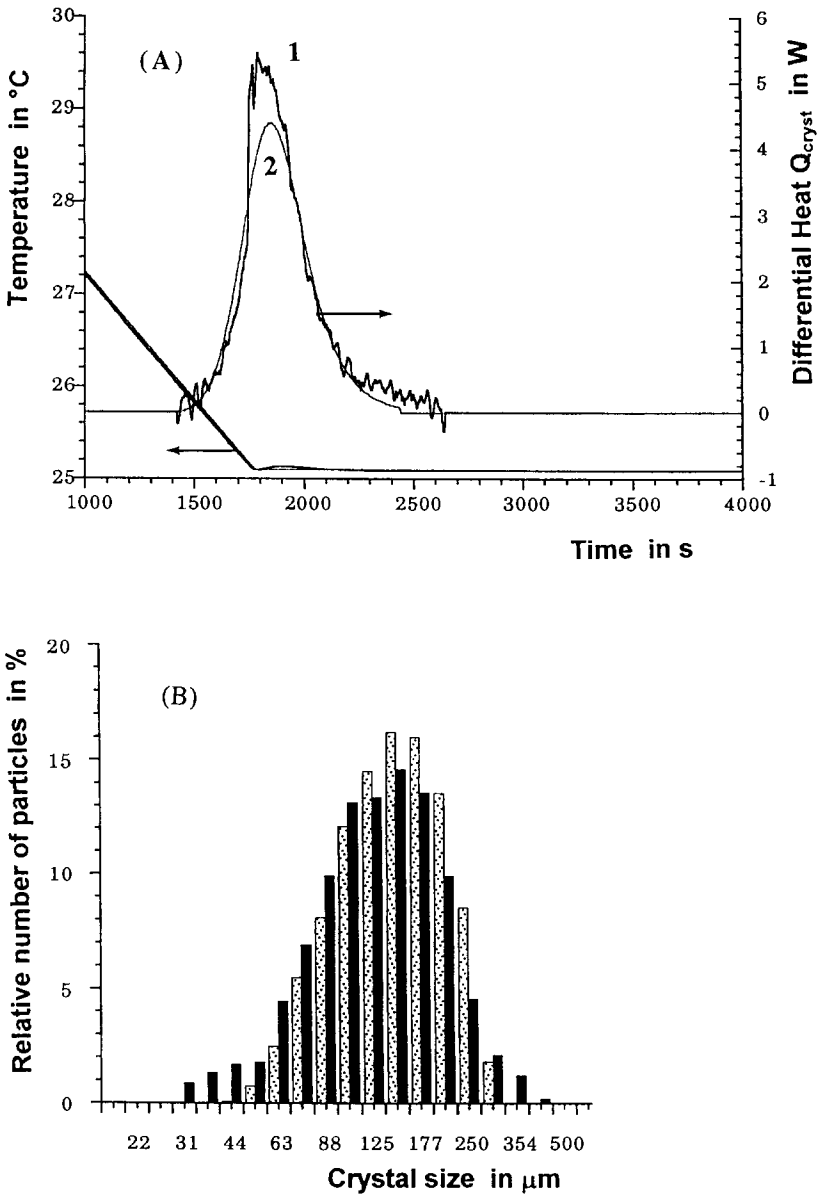

Fig. 6. Measurements and simulations of a batch crystallization of adipic acid in water. (A) Differential heat of crystallization Q_{cryst}: 1, calorimetric measurements; 2, simulation. (B) Final Image analysis (black) and simulated (dotted) CSD.

release during the different crystallization operations. As expected, parameters A and A_{sec} are found to be constant, while parameters B and B_{sec} appear to be temperature-dependent [19]. The following values are proposed, where θ is the absolute temperature. The growth parameters given in Ref. [18] were also applied to simulate the process

$$A = 1.8 \times 10^{10}\,[\text{nb}]\,\text{s}^{-1}\,\text{m}^{-3}; \quad A_{sec} = 1.37 \times 10^{15}\,[\text{nb}]\,\text{s}^{-1}\,\text{m}^{-3}\,\text{m}^{-2} \tag{15}$$

$$B = \frac{3.57 \times 10^{30}}{\theta^{12.7}} \quad \text{and} \quad B_{sec} = \frac{4.25 \times 10^{59}}{\theta^{24.8}} \tag{16}$$

Fig. 6 shows an example of the good agreement obtained between experimental results and simulations using the optimized set of kinetic parameters. As one can see, despite slight differences in the final CSD, the fitting of both calorimeteric and granulometric data is rather satisfactory. Identical performances of the simulation program were obtained with other runs which are not shown here.

5. Conclusion

It is well known that obtaining reliable and accurate measurements both during and after industrial crystallization operations is still difficult. The modelling of crystallization processes requires careful identification of the nucleation(s) and growth kinetics which can only be achieved if sufficient information is provided by the sensors that are used to characterize both the liquid phase and the granulometry of the particles. The goal of the present study was to use calorimetry as an indirect supersaturation sensor, together with on-line laser CSD measurements and final off-line image analyses of the produced particles. The method of classes was applied as an efficient technique for solving the population balance equations together with a specific kinetic modelling strategy.

Isothermal adipic acid/water crystallizations were performed in the Mettler RC1 reaction calorimeter in order to evaluate the method. These experiments allowed an estimation of a reliable set of kinetic parameters which were used to simulate the population balances. The agreement between experimental and simulated variables, such as the supersaturation, the heat release due to the crystal growth, and the final CSD, was found to be promising.

Nomenclature

A, B	empirical coefficients in the primary nucleation law, $A/[\text{nb}]\,\text{s}^{-1}\,\text{m}^{-3}$
A_{sec}, B_{sec}	empirical coefficients in the secondary nucleation law, $A_{sec}/[\text{nb}]\,\text{s}^{-1}\,\text{m}^{-5}$
C	solute concentration/mol m^{-3}
C^*	solubility/mol m^{-3}
$\mathscr{C}_i$	ith granulometric class
f_i	average value of ψ on $\mathscr{C}_i/[\text{nb}]\,\text{m}^{-1}\,\text{m}^{-3}$
G	growth rate/m s^{-1}

k_C	kinetic constant of the integration law/mol^{1-n} m^{3n-2} s^{-1}
k_d	mass transfer coefficient/m s^{-1}
L	characteristic size of crystals/m
L_i	upper bound of $\mathscr{C}_i$/m
$\mathscr{L}_i$	width of class $\mathscr{C}_i$/m
L_0	size of nuclei/m
M	molecular weight of solid/kg mol^{-1}
m_0	initial mass of dissolved solid/kg m^{-3}
m_C	mass of crystallized solid per unit volume of suspension/kg m^{-3}
n	integration kinetic order for the growth law
N	number of granulometric classes $\mathscr{C}_i$
N_T	total number of crystals/[nb]
N_i	number of crystals per unit volume of suspension in $\mathscr{C}_i$/[nb] m^{-3}
Q_{cryst}	instantaneous heat generation rate of crystallization/W
r_{N1}	primary heterogeneous nucleation rate/[nb] s^{-1} m^{-3}
r_{N2}	secondary nucleation rate/[nb] s^{-1} m^{-3}
S_p	total surface of particles/m^2
V_T	total volume of suspension/m^3

Greek letters

α_v, α_S	volumetric and surface shape factors
β	relative supersaturation C/C^*
ΔC	absolute supersaturation/mol m^{-3}
ΔH_C	crystallization enthalpy/J mol^{-1}
ψ	density function in the suspension/[nb] m^{-1} m^{-3}
Φ	flux density of the mass transfer/mol s^{-1} m^{-2}
ρ_S	density of the solid/kg m^{-3}

References

[1] T. Gutwald and A. Mersmann, Batch cooling crystallization at constant supersaturation: technique and experimental results, Chem. Eng. Technol., 13 (1990) 229–237.
[2] S.M. Miller and J.B. Rawlings, Model identification and control strategies for batch cooling crystallizers, AIChE J., 40(8) (1994) 1312–1327.
[3] Y. Qui and A.C. Rasmuson, Estimation of crystallization kinetics from batch cooling experiments, AIChE J., 40(5) (1994) 799–812.
[4] L. Hlozny, A. Sato and N. Kubota, On-line measurement of supersaturation during batch cooling crystallization of ammonium alum, J. Chem. Eng. Jpn., 25(5) (1992) 604–606.
[5] S.K. Sikdar and A.D. Randolph, Secondary nucleation of two fast growth systems in a mixed suspension crystallizer : Magnesium sulfate and citric acid water systems, AIChE J., 22(1) (1976) 110–117.
[6] R. Riesen, Optimization of industrial crystallization processes, Chem. Plants Process., July (1992) 26–29.
[7] A. König, H.H. Emons and V.L. Rylov, Calorimetric determination of the kinetic parameters of crystalization, Zh. Prikl. Khim., 63(10) (1990) 2231–2236.

[8] G. Févotte and J.P. Klein, Application of on-line calorimetry to the advanced control of batch crystallizers, Chem. Eng. Sci., 49(9) (1994) 1323–1336.
[9] G. Févotte and J.P. Klein, Crystallization calorimetry for the assessment of batch seeding and cooling policies, Chem. Eng. J., 59 (1995) 143–152.
[10] G. Févotte and J.P. Klein, A new policy for the estimation of the course of supersaturation in batch crystallization, Can. J. Chem. Eng. (1996), June, 74.
[11] J.B. Rawlings, W.R. Witkowski and J.W. Eaton, Modelling and control of crystallizers, Powder Technol., 69 (1992) 3–9.
[12] J.B. Rawlings, S.M. Miller and W.R. Witkowski, Model identification and control of solution crystallization processes : a review, Ind. Eng. Chem. Res., 32 (1993) 1275–1296.
[13] B. Singh, Using a crystal size distribution sensor to improve the operation and control of batch crystallizers, Anal. Proc., 30 (1993) 495–496.
[14] S.K. Heffels, E.J. de Jong and M. Nienoord, Improved operation and control of batch crystallizers, AIChE Symp. Ser., 87 (1991) 170–181.
[15] O. Monnier, J.P. Klein, C. Hoff and B. Ratsimba, Particle size determination by laser reflection — methodology and problems, Part. Part. Syst. Charact., 13 (1996) 10017.
[16] A. Mersmann, Fudamentals of Crystallization, in A. Mersmann (Ed.), Crystallization Technology Handbook, Marcel Dekker, Inc., New York, 1995.
[17] D.M. Levins and J.R. Glastonbury, Particle-liquid hydrodynamics and mass-transfer in a strirred vessel. Part II : Mass transfer, Trans. Inst. Chem. Eng., 50 (1972) 132–146.
[18] P. Marchal, R. David, J.P. Klein and J. Villermaux, Crystallization and precipitation engineering — I. An efficient method for solving population balance in crystallization with agglomeration, Chem. Eng. Sci., 43(1) (1988) 59–67.
[19] O. Monnier, G. Févotte, C. Hoff and J.P. Klein, Optimization of kinetic crystallization models by using coupled calorimetric and CSD measurements, 13th Symp. on Industrial Crystallization, Toulouse, France, September, (1996), preprints.